Development 138, 2631 (2011) doi:10.1242/dev.069096

The nucleoporin Seh1 forms a complex with Mio and serves an essential tissue-specific function in *Drosophila* oogenesis

Stefania Senger, John Csokmay, Tanveer Akbar, Takako Iida Jones, Prabuddha Sengupta and Mary A. Lilly

There was an error published in *Development* **138**, 2133-2142.

In the online version of the article published on 26th April 2011, Dr Tanveer Akbar's name appeared in reverse order (full text) or with an inappropriate comma (PDF).

The correct author list appears above. The printed version is correct.

We apologise to the authors and readers for this mistake.

Development 138, 2133-2142 (2011) doi:10.1242/dev.057372

The nucleoporin Seh1 forms a complex with Mio and serves an essential tissue-specific function in *Drosophila* oogenesis

Stefania Senger[1,*], John Csokmay[2], Tanveer, Akbar[1], Takako Iida Jones[1,*,†], Prabuddha Sengupta[1] and Mary A. Lilly[1,‡]

SUMMARY

The nuclear pore complex (NPC) mediates the transport of macromolecules between the nucleus and cytoplasm. Recent evidence indicates that structural nucleoporins, the building blocks of the NPC, have a variety of unanticipated cellular functions. Here, we report an unexpected tissue-specific requirement for the structural nucleoporin Seh1 during *Drosophila* oogenesis. Seh1 is a component of the Nup107-160 complex, the major structural subcomplex of the NPC. We demonstrate that Seh1 associates with the product of the *missing oocyte* (*mio*) gene. In *Drosophila*, *mio* regulates nuclear architecture and meiotic progression in early ovarian cysts. Like *mio*, *seh1* has a crucial germline function during oogenesis. In both *mio* and *seh1* mutant ovaries, a fraction of oocytes fail to maintain the meiotic cycle and develop as pseudo-nurse cells. Moreover, the accumulation of Mio protein is greatly diminished in the *seh1* mutant background. Surprisingly, our characterization of a *seh1* null allele indicates that, although required in the female germline, *seh1* is dispensable for the development of somatic tissues. Our work represents the first examination of *seh1* function within the context of a multicellular organism. In summary, our studies demonstrate that Mio is a novel interacting partner of the conserved nucleoporin Seh1 and add to the growing body of evidence that structural nucleoporins can have novel tissue-specific roles.

KEY WORDS: Seh1 (Nup44A), Mio, NPC, Nup107-160, Nucleoporin, Oogenesis, Meiosis, Germline, *Drosophila*, Mtor (Tpr), Microtubule

INTRODUCTION

The pathways that control progression through the early meiotic cycle remain poorly understood in metazoans. *Drosophila melanogaster* provides a genetically tractable system with which to study the relationship between early meiotic progression and oocyte development. As in mammals and *Xenopus*, the *Drosophila* oocyte initiates meiosis within the context of a germline cyst (de Cuevas et al., 1997; Pepling, 2006; Pepling et al., 1999). *Drosophila* ovarian cysts are produced through a series of four synchronous mitotic divisions during which cytokinesis is incomplete (de Cuevas et al., 1997; Huynh and St Johnston, 2004). Soon after the completion of the mitotic divisions, all 16 cells enter premeiotic S phase (Carpenter, 1981). However, only the true oocyte, which comprises one of the two cells at the center of the syncytium, remains in meiosis and goes on to produce a gamete. The other 15 cells lose their meiotic features, enter the endocycle, and develop as polyploid nurse cells. In contrast to the nurse cells, the single oocyte remains in prophase of meiosis I until it proceeds to the first meiotic metaphase late in oogenesis. The pathways that drive this complicated series of cell cycle transitions that are so critical to the development of the mature gamete remain a topic of great interest.

[1]Cell Biology and Metabolism Program, National Institute of Child Health and Human Development, National Institutes of Health, Bethesda, MD 20892, USA.
[2]Reproductive Biology and Medicine Program, National Institute of Child Health and Human Development, National Institutes of Health, Bethesda, MD 20892, USA.

*Present address: Mucosal Biology Research Center, University of Maryland School of Medicine, Baltimore, MD 21201, USA
†Present address: Boston Biomedical Research Institutes, Watertown, MA 02472, USA
‡Author for correspondence (mlilly@helix.nih.gov)

Accepted 15 March 2011

The *missing oocyte* (*mio*) gene was identified in a forward genetic screen for mutants affecting cell cycle regulation and oocyte differentiation in early ovarian cysts (Iida and Lilly, 2004). In *mio* mutants, the oocyte enters the meiotic cycle, forms mature synaptonemal complexes and accumulates oocyte-specific markers. However, in the absence of Mio, the oocyte fate is not stably maintained. Soon after the nurse cells enter the endocycle in stage 1 of oogenesis, *mio* oocytes follow the nurse cells into the endocycle, lose the preferential accumulation of oocyte-specific markers and develop as pseudo-nurse cells. Thus, *mio* is required for the maintenance of the meiotic cycle and oocyte identity. The *mio* gene encodes a 975 amino acid protein that is highly conserved from yeast to humans (Iida and Lilly, 2004). Yet, the molecular function of *mio* remains elusive. Here, we demonstrate that Mio associates with the conserved nucleoporin Seh1 (also known as Nup44A in *Drosophila*). Moreover, we define a tissue-specific requirement for Seh1 during oogenesis.

Seh1 is a component of a nucleoporin subcomplex known as the Nup107-160 complex in higher eukaryotes and the Nup84 complex in yeast (Fahrenkrog et al., 2004; Hetzer et al., 2005; Wozniak et al., 2010). The Nup107-160 complex, which is the major structural component of the nuclear pore complex (NPC), consists of at least nine subunits in higher eukaryotes and functions in the regulation of mRNA export as well as in the assembly and distribution of NPCs within the nuclear envelope (Hetzer et al., 2005; Wozniak et al., 2010). Studies over the last five years have defined several physiological functions for the Nup107-160/Nup84 complex that appear to be independent of nucleocytoplasmic transport (Fahrenkrog et al., 2004; Wozniak et al., 2010). Most notably, in *Xenopus* egg extracts and HeLa cells, the Nup107-160 complex has a dynamic localization during the cell cycle (Hetzer et al., 2005). Although present on the nuclear envelope in interphase, the entire complex targets to kinetochores, spindles and spindle poles to

varying extents during mitosis (Loiodice et al., 2004; Orjalo et al., 2006). Consistent with a mitotic function, depleting components of the Nup107-160 complex results in cell cycle abnormalities, including defects in mitotic spindle formation, chromosome segregation and cytokinesis (Orjalo et al., 2006; Platani et al., 2009). Moreover, recent evidence indicates that in HeLa cells and *Xenopus* egg extracts, the Nup107-160 complex mediates microtubule nucleation at kinetochores via its interaction with the γ-TuRC complex (Mishra et al., 2010). Unlike in other metazoans, in *Drosophila* Nup107 fails to localize to kinetochores at mitosis but is found concentrated in the spindle region (Katsani et al., 2008). In summary, the Nup107-160 complex is multifunctional, with roles in both nucleocytoplasmic transport and cell cycle regulation.

Here, we demonstrate that Mio, a protein that is required for maintenance of the meiotic cycle and oocyte fate during oogenesis, associates with the structural nucleoporin Seh1. Surprisingly, we find that a *seh1* deletion allele is viable but exhibits dramatically reduced female fertility. Closer examination reveals that, as is observed in *mio* mutants, in a fraction of *seh1* ovarian cysts oocytes fail to maintain the meiotic cycle and oocyte fate into later stages of oogenesis. From our studies we conclude that Seh1 has an essential germline function during oogenesis but is not required for the growth or development of somatic tissues.

MATERIALS AND METHODS

Drosophila strains and genetics

The mio^{1} and mio^{2} alleles were described previously (Iida and Lilly, 2004). The *Drosophila* stock carrying the *PBac{WH}f07552* insertion was obtained from the Harvard Exelixis Collection (Thibault et al., 2004). The *Drosophila* stock carrying the insertion $P\{RS3\}Nup44A^{CB-0750-3}$ was obtained from the Szeged Stock Center (Ryder et al., 2004). All additional stocks were provided by the Bloomington Stock Center or were generated as described below.

Generation of *seh1* deletion

A flipase recognition target (FRT) site-directed recombination was conducted to generate a deletion encompassing *seh1* coding sequence (CDS) using the Drodel Deficiency Kit (Bloomington Stock Center). The strains used were f07552a and CB-0750-3, each carrying single transposon insertions containing FRT sites located in the first intron and at the 3′ end of *seh1* (see Fig. S1 in the supplementary material). The FRT recombination was carried out as described (Golic and Golic, 1996). Two *seh1* deletions were generated: $seh1^{\Delta 15}$ and $seh1^{\Delta 86}$. The deletions were characterized by sequencing the FRT junction site and by PCR amplification of the *seh1* gene region in both the deleted and parental strains (data not shown). As predicted by the genome location of the transposons, we verified that the recombination generated a deletion of 2775 bp (from 3,876,949 to 3,879,724 bp) that includes the full *seh1* CDS (see Fig. S1 in the supplementary material). The described stocks are also referred to as w^{1118}; $seh1^{\Delta 15}$/*SM6a* and w^{1118}; $seh1^{\Delta 86}$/*SM6a* and represent null alleles of *seh1*. DNA oligos (5′ to 3′) for FRT junction analysis were: W11678u, TCATCGCAGATCAGAAGCGG; W5662-81, GTCTGGCCATTCTCATCGTGA; P{WH}3984-3959, TAATTCGGCTGCTGCTCTAAACGACG; and P{WH}4434-4409, CGTTTCGTAGTTGCTCTTTCGCTGTC.

cDNA and constructs

The full-length *mio* CDS was cloned in frame with a 5′ 1× FLAG and a 3′ HA tag into a pCRII-Topo vector (Invitrogen, Carlsbad, CA, USA) and subcloned into the pCaSpeR4 vector (EMBL Accession Number, X81645) downstream of a 1061 bp fragment encompassing the native *mio* promoter region.

The full-length cDNA SD07614 encoding the *seh1* gene was obtained from the Drosophila Genomics Resource Center (Indiana University, Bloomington, IN, USA).

The CDS of the *Drosophila seh1* gene was amplified by two consecutives PCR rounds to add a 5′ 1× FLAG and 3′ HA tag and the unique restriction sites *Kpn*I and *Xho*I at the 5′ end and *Not*I and *Hin*dIII at the 3′ end using the following sets of primers (5′ to 3′): NUP1Ff, AGGAGGGTACCCTCGAGATGGTCGACGTGGAACCC; NUP1Rv, GGTAAAGCTTTGCGGCCGCGTGCCACGGCACCTGGT; NUP2Ff, GACCATGGATTACAAGGATGATGATGATAAGGAGGGTACCCTCGAG; and NUP2Rv, TCTAGAAGCATAATCAGAACATCATAAGGGTAAAGCTTTGCGGCC. The PCR product was subcloned into the pTOPO Blunt cloning vector (Invitrogen) and sequenced.

The construct FLAG::seh1::HA was subcloned into the multiple cloning site (MCS) of the expression vector pAct5C (Krasnow et al., 1989) under the control of the promoter of the *Drosophila Act5C* gene.

The Cerulean (CeFP) CDS was amplified from the pCerulean-C1 vector (Clontech, Mountain View, CA, USA) using the following primers: CeFP-Ff, GCTAGCGCTACCGGTCGCCACCGGTCGCCACCAT; and CeFP-Rv, GTTATCTAGATCCGGTGGATCCCGGGCCCGCGGTA. The PCR product was cloned into the pTOPO Blunt vector, sequenced and further subcloned into the MCS of pAct5C in frame with the seh1::HA sequence.

CeFP::seh1::HA sequence was subcloned into the MCS of the vector pUASp (Rorth, 1998) using the unique restriction sites *Bam*HI and *Xba*I.

The mCherry CDS was amplified from the pmCherry-C1 expression vector (Clontech) using the following primers: mCherryATG, gccgGAATTCatggtgagcaagggcgaggaggata; and mCherry Rev, gccgGAATTCttacttgtacagctcgtccatgccgc. The PCR product was subcloned into pAct5C in frame with the construct seh1::HA.

P element-mediated transformation and rescue

The construct p{w^{1118}, UAS::CeFP::*seh1*::HA} was injected into a *white* background to generate transgenic flies (Duke University Model System Genomics Service, Durham, NC, USA). To rescue the *seh1* genetic defects, the CeFP::seh1::HA construct was expressed in the $seh1^{\Delta 15}$ null genetic background using the germline-specific driver nanos-Gal4::VP16 (Rorth, 1998).

Generation of Mio antibody

The full-length *mio* CDS was cloned into the MCS of the bacterial expression vector pET32a (Novagen) and expressed in *E. coli* BL21 cells. The protein was purified from bacterial inclusion bodies according to standard techniques and the antigen was used to produce rabbit Mio antiserum (Covance, Princeton, NJ, USA). The Mio antiserum was used for western blot analysis in the present study.

S2 cell culture and RNA interference

S2 cells were grown in ventilated plastic flasks in Schneider's *Drosophila* medium (Gibco-Invitrogen) supplemented with 10% inactivated fetal bovine serum at 25°C. RNA interference (RNAi) was carried out as described (Maiato et al., 2003).

The double-stranded (ds) DNA transcription was carried out using the MEGAscript T7 RNAi Kit and the dsRNA was purified using the MEGAclear Kit (Ambion-Applied Biosystems, Foster City, CA, USA) according to the manufacturer's protocols. The RNAi templates were generated by PCR amplification using the following primers:
MioRNAiFf,
taatacgactcactatagggATGAGCGGCAATACACACGGACTCA;
MioRNAiRv, taatacgactcactatagggGGCCGTCTCCTTGGGAACTCC;
NupRNAi#1Ff, taatacgactcactatagggagaCGACGTGGAACCCATTATTG;
NupRNAi#1 Rv, taatacgactcactatagggagaTGTTGCTAATCTCGTGCTGC;
NupRNAi#3Ff,
taatacgactcactatagggagaGCAGCACGAGATTAGCAACA;
NupRNAi#3Rv,
taatacgactcactatagggagaTAGTTCATTCGCCACAGACGC;
GFPRNAiFf,
taatacgactcactatagggagaTGAGCAAGGGCGAGGAGCTGTTCAC; and
GFPRNAiRv,
taatacgactcactatagggagaAGTTGTACTCCAGCTTGTGCCCCAG.

Immunostaining and imaging

Fixation and immunostaining of ovaries were performed as described (Grieder et al., 2000). Antibodies were used at the following dilutions: mouse anti-Orb 6H4, 1:100 (purified IgG, Developmental Studies Hybridoma Bank, University of Iowa, IA, USA); mAb414, 1:400 (Covance); mouse anti-GFP, 1:200 (Roche, Basel, Switzerland); mouse anti-Mtor, 1:100 (Qi et al., 2004); rabbit anti-dmNup153, 1:200 (Dimaano et al., 2001); and rabbit anti-dmNup107, 1:1000 (Katsani et al., 2008). Secondary antibodies were anti-rabbit and anti-mouse conjugated to Alexa Fluor 594 and Alexa Fluor 488 (Molecular Probes-Invitrogen) and used at 1:1000. Nuclei were visualized by staining the DNA with DAPI (Sigma-Aldrich, St Louis, MO, USA). Images were acquired using an Olympus FV1000 Fluoview laser-scanning confocal microscope (Olympus, Tokyo, Japan). Composite figures were prepared using Photoshop 7.0 and Illustrator (Adobe Systems, San Jose, CA, USA).

In situ hybridization

In situ hybridization was carried out as described (Tautz and Pfeifle, 1989). Sense and antisense probes were dUTP-Dig labeled by asymmetric PCR amplification of the fourth exon, which is common to all of the predicted transcripts, using the following primers: Seh1 Sense, GACGCC-ACGGACATCTCCAAG; and Seh1 Anti, TGCCACGGCACCT-GGTTGCCG.

Tandem affinity purification and mass spectrometry

Drosophila S2 cells were stably or transiently transfected with a plasmid expressing full-length *mio* tagged with FLAG and HA under the control of a 1061 bp region of the wild-type *mio* promoter. One liter of S2 cell culture was used for a large-scale tandem affinity purification protocol using the FLAG HA Tandem Affinity Purification Kit (Sigma-Aldrich) according to the manufacturer's instructions. A modified RIPA buffer was used for the extraction (see below). One liter of untransfected S2 culture was used as control. The immunopurified samples were loaded on a 4-12% SDS gradient gel (Invitrogen) and stained with Coomassie Blue; the visible bands were excised and analyzed by tandem mass spectrometry (MS/MS; Custombiologics, Ontario, Canada).

Western analysis

Proteins from ovaries or S2 cells were extracted in modified RIPA buffer (50 mM Tris-HCl pH 8.0, 150 mM NaCl, 0.5% sodium deoxycholate, 1.0% Nonidet P40, 0.4 mM EDTA) containing 1 mM PMSF and Protease Inhibitor Cocktail (Roche). The supernatants were resolved in a NuPage 4-12% polyacrylamide gradient gel (Invitrogen) and blotted onto a PVDF membrane using a semi-dry Trans-Blot system (BioRad, Hercules, CA, USA). Western blot analyses were carried out using standard techniques. Mio antiserum was used at 1:10,000, mouse anti-α-tubulin (Jackson ImmunoResearch) at 1:5000, mouse anti-GFP (Roche) at 1:3000 and anti-β-actin (AbCam) at 1:1000. Anti-mouse and anti-rabbit horseradish peroxidase-conjugated secondary antibodies (Jackson ImmunoResearch, West Grove, PA, USA) were used at 1:5000 and 1:10,000, respectively.

RESULTS

Mio interacts with the nucleoporin Seh1

To identify proteins that physically interact with Mio, we performed a large-scale immunoprecipitation of a tagged HA-Mio-FLAG protein from *Drosophila* Schneider 2 (S2) tissue culture cells (Fig. 1A). Tandem mass spectrometry was employed to analyze the immunoprecipitated proteins. From several independent experiments, one protein, the nucleoporin Seh1, consistently co-purified with Mio. Seh1 is a component of the Nup107-160 subcomplex (Loiodice et al., 2004). Intriguingly, Seh1 was the only nucleoporin identified in any of our immunoprecipitations of Mio. Moreover, we determined by western blot that Mio does not co-immunoprecipitate the nucleoporins Nup107 and Mtor (also known as Tpr) (data not shown). In the *Drosophila* genome, the *Nup44A* gene encodes the only homolog of *seh1*; we will refer to the *Nup44A* gene and Nup44A protein as *seh1* and Seh1.

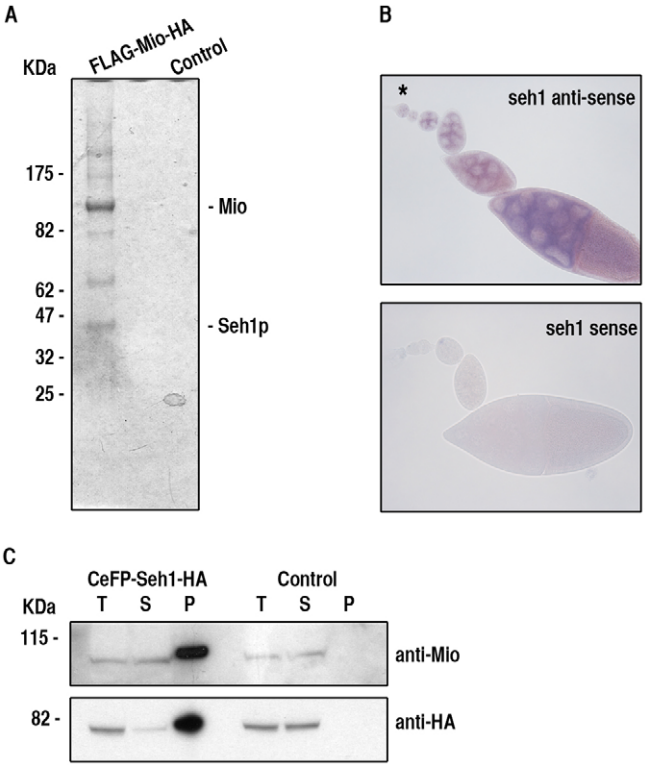

Fig. 1. Mio interacts with the nucleoporin Seh1. (**A**) Immunoprecipitation from S2 whole-cell lysates. *Drosophila* S2 cells were stably transfected with a vector containing FLAG- and HA-tagged *mio* coding sequence under the control of the wild-type *mio* promoter. Immunoprecipitates were run on an SDS-PAGE gel and stained with Coomassie Blue. The sample was compared with immunoprecipitates from non-transfected S2 cells (control). Tandem mass spectrometry was used to identify the co-precipitated proteins. Mio and Seh1 are indicated. (**B**) To verify the expression of *seh1* in the *Drosophila* germline, wild-type ovaries were labeled with antisense and sense *seh1* digoxigenin probes consisting of the *seh1-RB* fourth exon. Asterisk denotes the germarium. (**C**) Seh1 and Mio interact in the *Drosophila* germline. Immunoprecipitates are shown of total protein extracts from *Drosophila* ovaries expressing Seh1 under the control of the nanos-Gal4 driver. The immunoprecipitation was performed using an anti-GFP monoclonal antibody to pull down CeFP-Seh1-HA tagged protein. The immunoprecipitation of Seh1 was evaluated by western blot using antibodies against the HA tag. The levels of Mio protein were examined in total protein extracts (T), supernatant (S) and immunoprecipitated pellet (P). The control immunoprecipitation was performed using purified isotype-matched mouse IgG.

Consistent with a role for Seh1 in oogenesis, in situ hybridizations demonstrate that *seh1* is transcribed in developing ovarian cysts (Fig. 1B). Additionally, microarray analysis indicates that *seh1* is transcribed at moderate levels in nearly all tissues (Chintapalli et al., 2007). In order to determine the subcellular localization of the Seh1 protein, we generated a transgenic line that expressed a tagged Seh1 protein under the control of an inducible promoter (UASp::CeFP::Seh1::HA). As described below, the CeFP-Seh1-HA protein is fully functional as measured by the ability of the transgene to rescue a *seh1* null allele. As anticipated for a nucleoporin, when expressed in the female germline CeFP-Seh1-HA was enriched on the nuclear envelope of the nurse cells and oocyte (see Fig. S2 in the supplementary

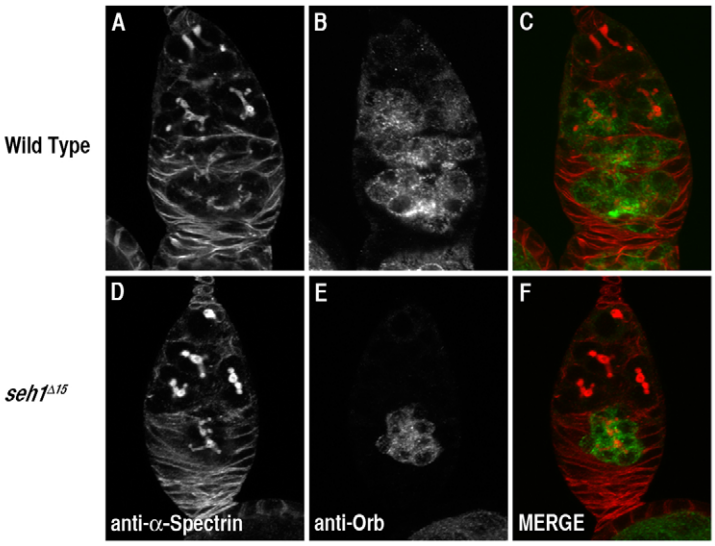

Fig. 2. *seh1*$^{\Delta 15}$ germaria have reduced numbers of ovarian cysts. (**A-F**) Wild-type (A-C) and *seh1*$^{\Delta 15}$ (D-F) *Drosophila* germaria stained with anti-α-Spectrin to visualize the fusome (A,D; red in C,F) and anti-Orb to visualize ovarian cysts that have entered the meiotic cycle (B,E; green in C,F). Note that the *seh1*$^{\Delta 15}$ germaria have a reduced number of Orb-positive ovarian cysts relative to wild type.

material). Similarly, the CeFP-Seh1-HA protein localized to the nuclear envelope in syncytial embryos as well as in somatically derived S2 tissue culture cells (see Fig. S2 in the supplementary material; data not shown). However, unlike the behavior of Seh1 in *Xenopus* and mammals, in *Drosophila* CeFP-Seh1-HA did not accumulate on kinetochores in mitosis (data not shown). The absence of detectable levels of Seh1 at kinetochores is consistent with the pattern of localization reported for another *Drosophila* component of the Nup107-160 complex, Nup107 (Katsani et al., 2008). Finally, we confirmed that Mio and Seh1 interact in the female germline. We expressed the CeFP-Seh1-HA protein in the female germline by means of the nanos-Gal4 driver. An anti-GFP antibody was used to immunoprecipitate the CeFP-Seh1-HA protein. In this experiment, endogenous Mio protein co-precipitated with CeFP-Seh1-HA (Fig. 1C). Together, our data indicate that Mio associates with the nucleoporin Seh1 in both germline and somatic tissues.

Seh1 is required for oogenesis but is dispensable for somatic development

To fully assess the role of Seh1 in vivo we generated a *seh1* null allele. *seh1* is predicted to encode three transcripts of 2401 nt (*seh1-RA*), 1284 nt (*seh1-RB*) and 1332 nt (*seh1-RC*) (FBgn0033247). All three predicted transcripts contain the same open reading frame (ORF), which encodes a protein of 354 amino acids (see Fig. S1 in the supplementary material). To generate a *seh1* null allele we made a 2775 bp deletion that removes the entire *seh1* ORF (see Materials and methods for details). The deletion does not extend into adjacent genes (see Fig. S1 in the supplementary material). Two independent isolates of the *seh1* deletion, *seh1*$^{\Delta 15}$ *and seh1*$^{\Delta 86}$, were generated. The phenotypes of the independent *seh1*$^{\Delta}$ isolates were indistinguishable. For the majority of the studies described here, we used the *seh1*$^{\Delta 15}$ deletion. Surprisingly, *seh1*$^{\Delta 15}$mutants were homozygous viable and eclosed at nearly Mendelian ratios. However, *seh1*$^{\Delta 15}$ homozygous females exhibited markedly reduced fecundity, laying just one-quarter the eggs of wild-type controls. Moreover, the eggs laid by *seh1*$^{\Delta 15}$ females hatched at ~40% of the rate of those laid by age-matched wild-type controls (n>280). Importantly, the reductions in *seh1*$^{\Delta 15}$ fertility, as well as the specific oogenesis defects described below, were rescued when the tagged *seh1* transgene was expressed using the germline-specific driver nanos-Gal4. Thus, the fertility defects observed in *seh1*$^{\Delta 15}$ females are due to the absence of the *seh1* gene product in the germline.

The *Drosophila* ovary comprises 16-20 ovarioles. Individual ovarioles are composed of a germarium, which contains germline and somatic stem cells, followed by a series of egg chambers at successively older stages of development. The germarium, which is present at the anterior tip of the ovariole, is divided into three regions. In region 1 (R1), incomplete mitotic divisions result in the production of the 16-cell interconnected germline cyst. Individual cells within the ovarian cyst are referred to as cystocytes. In region 2a (R2a), all 16 cells enter meiosis and undergo premeiotic S phase. Subsequently, in late R2a, a meiotic gradient forms as the cells near the center of the cyst, construct synaptonemal complexes and accumulate oocyte markers. As cysts progress down the germarium into region 2b (R2b) and beyond, the meiotic cycle is restricted to the single oocyte. Finally, in region 3 (R3), just prior to when the fully formed egg chamber buds off from the germarium, the nurse cells enter the endocycle while the oocyte remains in prophase of meiosis I.

To better understand the role of *seh1* in oogenesis, we labeled *seh1*$^{\Delta 15}$ and wild-type ovaries with several markers that allowed us to follow oocyte development and meiotic progression. Mutant and wild-type ovaries were dissected, fixed and stained with DAPI and with antibodies against Orb, a germline-specific protein that is expressed at high levels in post-mitotic ovarian cysts, and against α-Spectrin, a component of the actin cytoskeleton (de Cuevas et al., 1996; Lantz et al., 1994; Page and Hawley, 2001). Consistent with reduced fertility, *seh1*$^{\Delta 15}$ ovarioles contained fewer egg chambers and exhibited smaller germaria than ovarioles from wild-type females (Fig. 2).

To follow the mitotic cyst division in R1 of the germarium, we examined fusome morphology. The fusome is a germline-specific organelle, rich in actin cytoskeletal proteins, that forms along the remnants of the mitotic spindles to connect all cells within mitotically active ovarian cysts (de Cuevas et al., 1997; McKearin, 1997). The branching pattern of this unique germline organelle can be used to identify ovarian cysts in the mitotic cycle (de Cuevas et al., 1996; de Cuevas and Spradling, 1998; Grieder et al., 2000; Lin et al., 1994). Analysis of fusome morphology in *seh1*$^{\Delta 15}$ germaria using anti-α-Spectrin revealed that the number and distribution of

Table 1. Germline cysts per germarium

Genotype	No. of germaria	Stem cells	R1 cysts	R2a cysts	R2b cysts	R3 egg chamber
Wild type	16	2.0±0.0	4.2±1.0	3.7±0.7	2.5±1.0	1.0±0.0
seh1$^{\Delta 15}$	23	2.0±0.0	5.3±0.9	0.8±0.8	0.6±0.7	0.7±0.4

mitotic cysts in R1 were similar to those of wild-type ovaries (Fig. 2 and Table 1). By contrast, *seh1*$^{\Delta 15}$ germaria showed a dramatic decrease in the number of Orb-positive post-mitotic (16-cell) cysts in R2 and R3. Whereas control germaria had approximately seven post-mitotic cysts per germarium, *seh1*$^{\Delta 15}$ females contained on average only two post-mitotic cysts, a ~70% reduction (Table 1). Thus, *seh1*$^{\Delta 15}$ germaria contain wild-type numbers of mitotic ovarian cysts but have a reduction in the number of post-mitotic cysts.

seh1^{null} females produce egg chambers with 16 nurse cells and no oocyte

We find that in both *seh1*$^{\Delta 15}$ homozygous (n=509) and *seh1*$^{\Delta 15}$/*Df(2R)ED1735* transheterozygous (n=119) females, ~20% of egg chambers develop with 16 polyploid nurse cells and no oocyte (Fig. 3A-D and Table 2). Thus, *seh1* influences oocyte development. Intriguingly, failure to maintain the meiotic cycle and oocyte identity is the primary phenotype observed in *mio* ovaries

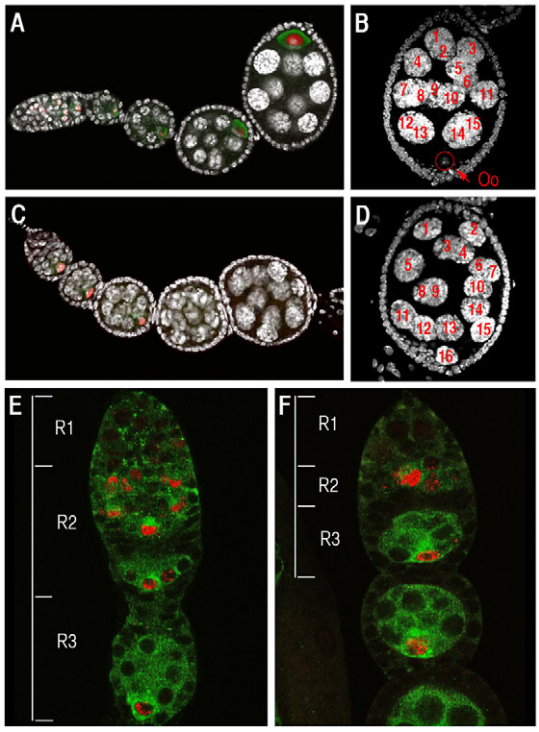

Fig. 3. *seh1* promotes the maintenance of the oocyte fate. (**A**,**C**) Wild-type (A) and *seh1*$^{\Delta 15}$ (C) *Drosophila* ovarioles stained with DAPI and the oocyte markers anti-C(3)G (red) and anti-Orb (green). Note that in a fraction of egg chambers from *seh1*$^{\Delta 15}$ ovarioles the oocyte becomes polyploid. (**B**) A wild-type stage 6 egg chamber that contains 15 polyploid cells. Arrow indicates the oocyte (Oo) DNA that has condensed into a compact karyosome (circled). (**D**) A *seh1*$^{\Delta 15}$ stage 6 egg chamber that contains 16 polyploid cells and no apparent oocyte. (**E**,**F**) Germarium from wild-type (E) and *seh1*$^{\Delta 15}$ homozygous (F) females stained with anti-Orb (green) and anti-C(3)G (red) antibodies. R1, R2 and R3 denote the regions of the germarium.

(Iida and Lilly, 2004). We wanted to determine whether *seh1* ovarian cysts fail to enter the meiotic cycle in the germarium or, alternatively, if mutant oocytes enter meiosis but fail to maintain the meiotic cycle into later stages of oogenesis. In order to distinguish between these two possibilities, we followed meiotic progression using an antibody against the synaptonemal complex protein C(3)G (Page and Hawley, 2001). As is observed in both wild-type and *mio* egg chambers, *seh1* ovarian cysts entered the meiotic cycle with a fraction of cystocytes progressing to pachytene, as measured by the construction of a mature synaptonemal complex (Fig. 3E,F). However, in ~20% of *seh1* egg chambers, the oocyte failed to maintain the meiotic cycle and instead entered the endocycle and developed as a pseudo-nurse cell (Fig. 3B,D). Thus, mutations in *seh1* disrupt the ability of the oocyte to maintain the meiotic cycle beyond the germarium.

Maintenance of the meiotic cycle and oocyte identity require the directional transport of proteins and mRNAs from the nurse cells to the oocyte along a polarized microtubule network (reviewed by Huynh and St Johnston, 2004). We examined the distribution of the Orb protein in wild-type and *seh1* developing ovarian cysts. During the early meiotic cycle, the distribution of Orb is dynamic (Christerson and McKearin, 1994; Lantz et al., 1994). In wild-type ovarian cysts, Orb localization starts out relatively homogenous in R2a. However, as cysts travel down the germarium the Orb protein accumulates in a single centrally localized cell, such that by late R2b, high levels of Orb are restricted to the anterior cortex of the presumptive oocyte. Subsequently, in R3, just prior to when the egg chambers bud off from the germarium, the focus of Orb staining follows the microtubule-organizing center (MTOC) and translocates from the anterior to the posterior of the oocyte. We found that in over 25% of *seh1*$^{\Delta 15}$ovarian cysts (n>128), the preferential accumulation of Orb to the oocyte was delayed and/or otherwise aberrant. Additionally, in *seh1* mutants the focus of Orb staining often failed to translocate to the posterior of the oocyte in R3, with older egg chambers retaining an anterior localization of Orb (see Fig. S3 in the supplementary material). The dynamic localization of Orb during oogenesis requires a polarized network of microtubules to be established and maintained in developing ovarian cysts (Theurkauf et al., 1993). Thus, our data suggest that the regulation of microtubule dynamics and/or function might be aberrant in a fraction of *seh1*$^{\Delta 15}$ ovarian cysts.

An additional marker for the regulation of microtubule organization and function in ovarian cysts is the dynamic behavior of the nurse cell centrioles in R2 and R3 of the germarium. After completion of the mitotic cyst divisions, the nurse cell centrioles dissociate from the nuclear membrane and migrate along the fusome towards the oocyte (Mahowald and Strassheim, 1970). By R3, most of the centrioles have completed this migration and are located in a loose cluster near the anterior of the oocyte nucleus. Subsequently, the centrioles migrate to the newly formed MTOC near the posterior of the oocyte (Huynh et al., 2001b; Huynh and St Johnston, 2004) (Fig. 4A). We found that in a fraction of *seh1*$^{\Delta 15}$ egg chambers, the centrioles failed to undertake this essential migration (Fig. 4B). By examining older *seh1*$^{\Delta 15}$ egg chambers, we observed that the failure of centrioles to migrate correlates with entry into the endocycle and the loss of the oocyte fate. Similarly,

Table 2. *seh1* dominantly suppresses the *mio* 16-nurse-cell phenotype

Maternal genotype	*n*	16 NC (%)	Wild type (%)	Others (%)
w; mio^{2}/mio^{1}	119	95.4	2.4	2.2
*w; mio^{2}/Df(2L)Exel6007**	123	75.3	11.2	3.5
w; mio^{1}/Df(2L)Exel6007	155	69.5	20.5	10.0
w; mio^{2}, seh1$^{\Delta 15}$	265	19.8	75.7	4.5
w; mio^{2}, seh1$^{\Delta 15}$/mio^{1}	178	27.2	72.8	0.0
w; mio^{2}, seh1^{EP2417}/mio^{1}	120	45.3	42.5	12.2
w; mio^{2}, Df(2R)ED1735†/mio^{1}	186	2.1	97.9	0.0
w; mio^{2}, Df(2R)ED1735/Df(2L)Exel6007	166	13.2	83.6	3.2
w; mio^{1}, Df(2R)ED1735/Df(2L)Exel6007	135	2.2	96.3	1.5

NC, nurse cell.
**Df(2L)Exel6007* encompasses the *mio* CDS.
†*Df(2R)ED1735* encompasses the *seh1* CDS.

in *mio* egg chambers the centrioles failed to undertake this crucial migration (Fig. 4C). Taken together, these data suggest that Seh1 might influence the maintenance of the meiotic cycle and oocyte identity by regulating the construction and maintenance of the polarized microtubule network within the developing oocyte. Consistent with this hypothesis, in *seh1* and *mio* egg chambers the distribution of microtubules was frequently disorganized, with mutant egg chambers lacking the posterior accumulation of microtubules that marks the MTOC in wild-type egg chambers (Fig. 4D-F).

In mammalian cells, reducing the levels of Seh1, or other Nup107-160 complex members, results in spindle defects and mitotic delay (Mishra et al., 2010; Platani et al., 2009; Zuccolo et al., 2007). Additionally, *Xenopus* egg extracts depleted of Nup107-160 complex members have a reduced ability to assemble bipolar spindles (Mishra et al., 2010; Orjalo et al., 2006). Therefore, we examined whether mutations in *seh1* alter mitotic progression during oogenesis, which might partially account for the reduced fecundity of *seh1$^{\Delta 15}$* females, by staining *seh1$^{\Delta 15}$* and wild-type ovaries with antibodies against Histone H3 phosphorylation at serine 10 (PH3), which serves as a marker for cells in mitosis (Hendzel et al., 1997). We counted the number of germaria that contained at least one PH3-positive ovarian cyst in R1. Although *seh1$^{\Delta 15}$* and wild-type germaria had similar numbers of ovarian cysts in R1, *in seh1$^{\Delta 15}$* germaria about twice as many ovarian cysts were positive for PH3, indicating that they spend a greater proportion of their time in mitosis: 43.1±3.9% (n=117) of *seh1$^{\Delta 15}$* germaria versus 20.7±7.1% (n=168) of wild-type germaria had at least one PH3-positive cyst (P<0.001). Thus, *seh1* mutants exhibit a mitotic delay during the ovarian cyst divisions.

Seh1 promotes the accumulation of Mio protein

We analyzed the levels of Mio in total protein extracts from wild-type and *seh1* ovaries by western blot (Fig. 5A). Mio protein levels were reduced in ovarian extracts in two independent *seh1* mutant backgrounds: the null allele *seh1$^{\Delta 15}$* and the hypomorph *seh1^{EP2417}*. Notably, the decrease in Mio protein levels in the extracts from *seh1$^{\Delta 15}$* mutants was significantly greater than that observed with the hypomorphic *seh1* allele (Fig. 5). Consistent with the western blot analysis, immunostaining revealed that the levels of Mio protein were reduced and/or dispersed in *seh1$^{\Delta 15}$* ovarian cysts (data not shown). Finally, targeting the *seh1* transcript using two different RNAi constructs in S2 tissue culture cells dramatically reduced the levels of Mio protein (Fig. 5B). Specifically, 48 hours after targeting the *seh1* transcript by RNAi, the level of Seh1 and Mio proteins were decreased in both *seh1* RNAi samples relative to mock-treated cells. From these data, we conclude that Seh1 promotes the accumulation of Mio in both germline and somatic tissues of *Drosophila*. Although the loss of Seh1 reduced Mio protein levels, overexpression of Seh1 was not sufficient to increase the levels of Mio protein (see Fig. S4 in the supplementary material). These data indicate that Seh1 is necessary but not sufficient for the accumulation of Mio.

seh1 suppresses the *mio* 16-nurse-cell phenotype

To better define the relationship between *mio* and *seh1*, we examined whether the genes interact genetically. Surprisingly, we found that *seh1* acts as a strong dominant suppressor of *mio*. Specifically, the percentage of *mio* mutant egg chambers with an oocyte increased 6-fold when a single copy of the *seh1$^{\Delta 15}$* allele, or a larger deletion of the *seh1* genomic region, was present in the *mio* mutant background (Table 2 and Fig. 6D). Indeed, even a single copy of the *seh1^{EP2417}* hypomorphic allele partially suppressed the *mio* phenotype. In *mio* single mutants, the vast majority of egg chambers arrested prior to stage 5 of oogenesis, well before the

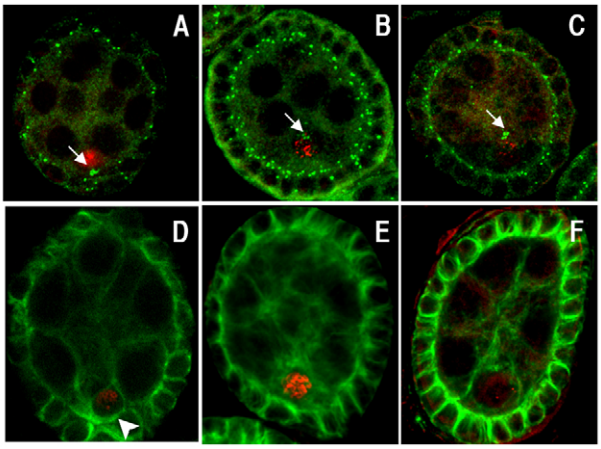

Fig. 4. Seh1 and Mio influence the translocation of the centrioles to the posterior of the oocyte. (**A-F**) Wild-type (A,D), *seh1$^{\Delta 15}$* (B,E) and *mio^{2}* (C,F) *Drosophila* egg chambers stained with anti-C(3)G (red) and anti-γ-Tubulin (green) to mark centrioles (A-C, arrows). Egg chambers in D-F are stained with anti-C(3)G (red) and anti-α-Tubulin (green) to mark microtubules. Note that in *seh1$^{\Delta 15}$* (B) and *mio^{2}* (C) egg chambers, the centrioles fail to migrate to the posterior of the oocyte. In wild-type egg chambers (D), microtubules accumulate in a crescent at the posterior of the oocyte (arrowhead). This posterior accumulation is often lacking in oocytes from *seh1* (E) and *mio* (F) egg chambers.

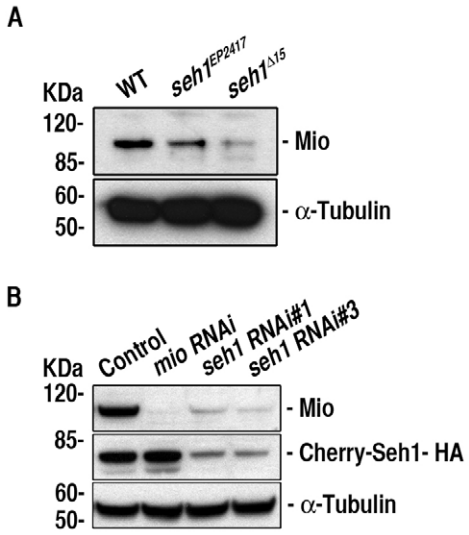

Fig. 5. Seh1 promotes the accumulation of Mio. (**A**) Western blot examining Mio levels from total protein extracts of wild-type (WT), hypomorphic *seh1*^{EP2417} and null *seh1*$^{\Delta 15}$ flies. α-Tubulin serves as a loading control. Note that the reduction of Mio protein reflects the severity of the *seh1* alleles. (**B**) A reduction in Mio protein is also observed in S2 tissue culture cells after RNAi against the *seh1* transcript. Two independent *seh1* RNAi targets were used, both of which reduced Mio protein levels compared with the control, which employed a sequence directed against GFP.

start of vitellogenesis in stage 7 (Fig. 6C) (Iida and Lilly, 2004). By contrast, egg chambers from *mio, seh1*/*mio,*+ females frequently progressed through vitellogenesis to produce mature eggs (Table 2 and Fig. 6D). Moreover, a small percentage of the eggs laid by *mio, seh1*$^{\Delta 15}$*/mio,*+ females hatched and developed into viable adults. Interestingly, reducing the dose of *mio* did not affect the ovarian phenotype of *seh1* (data not shown). Finally, we found that ovaries from *mio*^{2}*, seh1*$^{\Delta 15}$ females closely resembled those from *seh1*$^{\Delta 15}$ single mutants, with 80% of egg chambers containing an oocyte and 20% containing 16 nurse cells and no obvious oocyte (Table 2). These data strongly suggest that *seh1* is epistatic to *mio* with respect to the 16-nurse-cell phenotype. However, we note that ovaries from *mio*^{2}*, seh1*$^{\Delta 15}$ double homozygotes have fewer older egg chambers than *seh1*$^{\Delta 15}$ single mutants, suggesting that *mio* might have functions that are independent of *seh1*.

Mtor distribution is altered in *seh1* early meiotic cysts

In mammalian tissue culture cells, reducing the levels of Seh1 results in the partial redistribution of multiple nucleoporins from the NPC to cytoplasmic foci (Cordes et al., 1997; Loiodice et al., 2004). In order to determine whether Seh1 directs the recruitment of nucleoporins to the NPC in *Drosophila*, we examined the subcellular distribution of Nup107, Nup153 and Mtor, as well as the Phe-Gly (FG) repeat-containing nucleoporins in *seh1* mutant ovaries (Katsani et al., 2008; Mendjan et al., 2006; Qi et al., 2004). Notably, in both the somatic and germline cells of *seh1* mutant ovaries, the distribution of Nup107, a core component of the Nup107-160 complex, was indistinguishable from that of the wild type in both germline and somatic tissues (Fig. 7D,E). Similarly, the distribution of the FG-containing nucleoporins, which line the inner channel of the NPC, as well as that of Nup153 appeared unaffected in the *seh1* background (Fig. 7F,G; data not shown). Moreover, we determined that Mio does not co-immunoprecipitate Nup107, Nup153 or Mtor (data not shown). Thus, as suggested by our phenotypic analysis as well as by work in other organisms, Seh1 does not play a major role in the recruitment of nucleoporins to the NPC.

Although Mio does not physically associate with the nucleoporin Mtor, we found that mutations in *seh1* alter the distribution of Mtor in the female germline, most notably as cysts enter the meiotic cycle beginning in R2a of the germarium (Fig. 6B,C; data not shown). In interphase cells, Mtor is found on the inner face of the NPC in a structure called the nuclear basket, as well as in the nucleoplasm (Krull et al., 2004; Hase and Cordes, 2003). In wild-type females, Mtor has an interphase-like distribution in ovarian cysts in R2a, R2b and R3 of the germarium (Fig. 7A). However, in *seh1* ovarian cysts, there was a 20% displacement of Mtor from the nuclear envelope to the nucleoplasm (Fig. 7 and see Fig. S5 in the supplementary material). Thus, mutations in *seh1* alter the distribution of the nucleoporin Mtor during the early meiotic cycle in *Drosophila* females.

DISCUSSION

Here, we demonstrate a surprising tissue-specific requirement for the structural nucleoporin Seh1 in the female germline. We show that Seh1 associates with Mio, a highly conserved protein that is required for maintenance of the meiotic cycle and oocyte identity in *Drosophila*. Like *mio*, *seh1* has a crucial germline function during oogenesis. Moreover, our characterization of a *seh1* null allele indicates that, although required in the female germline, *seh1*

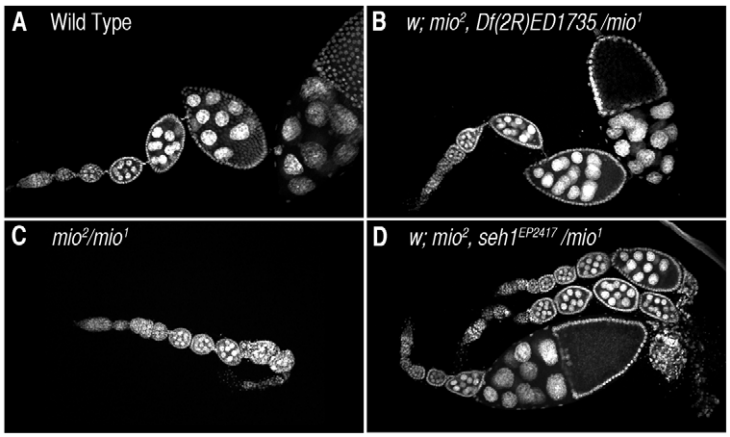

Fig. 6. *mio* genetically interacts with *seh1*. (**A**) Wild-type, (**B**) *w; mio*^{2}*, Df(2R)ED1735/mio*^{1}, (**C**) *mio*^{2}*/mio*^{1} and (**D**) *w; mio*^{2}*, seh1*^{EP2417}*/mio*^{1} *Drosophila* ovarioles stained with DAPI to visualize nuclei. In C and D, the *mio*^{2} ovarian phenotype is dominantly suppressed by mutations in *seh1*.

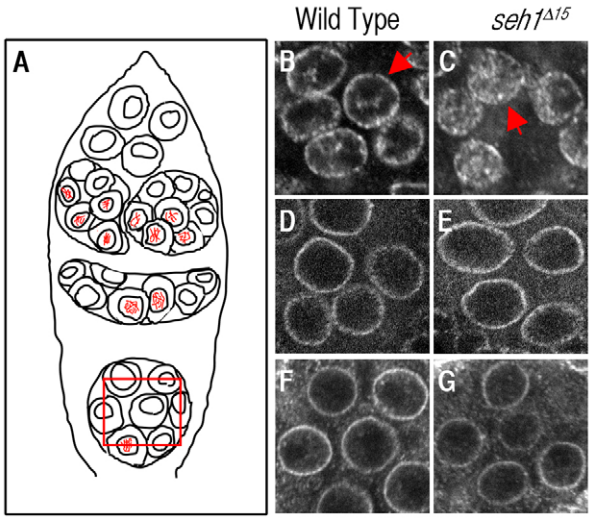

Fig. 7. The distribution of the nucleoporin Mtor is altered in the *seh1* mutant germline. (**A**) Schematic representation of a *Drosophila* germarium. Red lines indicate SC. The red box highlights nuclei analyzed by immunostaining in B-G. (**B-G**) Mtor (B,C), Nup107 (D,E) and Nup153 (F,G) immunostaining of germline nuclei in wild type (B,D,F) and $seh1^{\Delta 15}$ (C,E,G). Only the distribution of Mtor (arrows) is affected in the $seh1^{null}$ genetic background.

is dispensable for the development of somatic tissues. Our work represents the first examination of *seh1* function within the context of a multicellular organism.

To better understand how Mio influences the maintenance of the meiotic cycle and oocyte fate in *Drosophila*, we identified proteins that co-purify with Mio by tandem affinity purification. From these experiments, we determined that Mio is present in a stable complex with the structural nucleoporin Seh1. Seh1 is a component of the Nup107 complex, which is the primary structural unit of the nuclear pore. Studies in multiple organisms indicate that, although Seh1 is a nucleoporin, it is not required for bulk nucleocytoplasmic transport and has a limited role in the localization of other nucleoporins to the NPC (Loiodice et al., 2004; Orjalo et al., 2006). In contrast to its limited role at the NPC during interphase, recent evidence indicates that Seh1 has an essential function during mitosis. In *Xenopus* egg extracts and mammalian tissue culture cells, a fraction of the Nup107 complex that includes Seh1 targets to kinetochores, spindles and/or spindle poles from early prometaphase through early anaphase (Belgareh et al., 2001; Orjalo et al., 2006). Moreover, reducing the levels of Nup107-160 components disrupts spindle assembly and cytokinesis (Aitchison et al., 1995; Bai et al., 2004; Mishra et al., 2010; Orjalo et al., 2006; Platani et al., 2009; Zuccolo et al., 2007). Importantly, the specific depletion of *seh1* results in the failure of the Nup107 complex to target to kinetochores at mitosis and results in multiple mitotic defects (Zuccolo et al., 2007; Platani et al., 2009). Thus, Seh1 plays a role in the construction and/or maintenance of bipolar spindles in multiple organisms.

To define the role of Seh1 in *Drosophila* we generated a $seh1^{null}$ deletion allele. Considering the key role of Seh1 during mitosis in other organisms, we were surprised to find that $seh1^{null}$ homozygotes are viable. From this observation we conclude that *seh1* is dispensable in *Drosophila* for the mitotic cycle during the majority of somatic divisions. Consistent with a limited role for Seh1 during the mitotic cycle, we did not observe the specific accumulation of Seh1 on kinetochores during mitosis. Although this might reflect a limitation of our reagents, these data are in agreement with previous work demonstrating that the core component of the Nup107-160 complex, the nucleoporin Nup107, fails to accumulate at kinetochores during mitosis in multiple *Drosophila* tissues (Katsani et al., 2008).

Our studies also suggest a limited and/or redundant role for Seh1 in supporting the general structure and/or function of the NPC in interphase cells. Specifically, we find that multiple nucleoporins, including Nup107, target to the NPC in the absence of Seh1 in both germline and somatic tissues. The only nucleoporin mislocalization observed in $seh1^{null}$ mutants involved a limited displacement of Mtor from the nuclear envelope to the nucleoplasm in meiotic cysts in the germarium. Mtor is a component of the nuclear basket and is present on the cytoplasmic face of the NPC during interphase but relocates to the spindle matrix during mitosis (Lince-Faria et al., 2009; Qi et al., 2004). Whether the partial displacement of Mtor in the *seh1* background reflects a direct role for Seh1 in recruiting and/or stabilizing Mtor at the NPC remains to be determined.

Although dispensable for somatic development, we find that *seh1* has an essential function in the female germline during oogenesis. $seh1^{null}$ females are nearly sterile, producing only a small number of adult progeny. Indeed, $seh1^{null}$ females lay fewer eggs and contain ovarioles with a diminished number of egg chambers relative to wild-type females. A possible contributory factor to this reduced egg production is the mitotic delay observed during the ovarian cyst divisions. We find that in ovaries from *seh1* females, stem cells and ovarian cysts in R1 of the germarium spend a greater proportion of their time in mitosis than those in wild-type females. This phenotype is consistent with the metaphase delay observed in mammalian cells and *Xenopus* egg extracts depleted of members of the Nup107-160 complex, including Seh1. Thus, mutations in *seh1* alter the rate of egg chamber production, as well as the nature of the ovarian cyst divisions in the germarium.

In addition to affecting the overall rate of egg production, Seh1 influences the differentiation of the oocyte within the ovarian cyst. We demonstrate that, similar to what is observed in *mio* mutants, in a fraction of *seh1* ovarian cysts the oocyte enters the endocycle and develops as a pseudo-nurse cell. This does not reflect an inability of $seh1^{null}$ oocytes to enter the meiotic cycle. On the contrary, $seh1^{null}$ ovarian cysts enter the meiotic cycle on schedule with the two pro-oocytes progressing to pachytene, as measured by the construction of a mature synaptonemal complex. However, soon after exiting the germarium, a fraction of *seh1* mutant oocytes enter the endocycle and become polyploid. In *Drosophila*, oocyte differentiation, as well as the maintenance of the meiotic cycle, are contingent on the microtubule-based transport of mRNAs and proteins from the nurse cells to the oocyte (Huynh and St Johnston, 2004). The germline-specific RNA-binding protein Orb starts to accumulate in the oocyte in late R2a of the germarium. Defects that impair the microtubule-dependent accumulation of Orb in the oocyte correlate with the inability to maintain the meiotic cycle through later stages of oogenesis (Cox et al., 2001a; Cox et al., 2001b; Dienstbier et al., 2009; Fichelson et al., 2010; Hong et al., 2003; Huynh et al., 2001a; Huynh et al., 2001b; Huynh and St Johnston, 2000; Navarro et al., 2004; Roper and Brown, 2004). We find that in *seh1* ovarian cysts, the specific accumulation of Orb in the oocyte, as well as the secondary migration of Orb protein from the anterior to the posterior of the oocyte, are often delayed and/or otherwise defective. Additionally, the microtubule-dependent translocation of centrioles from the anterior to the posterior of the oocyte nucleus in the stage 1 oocyte is defective in both *mio* and

seh1 ovarian cysts. Thus, as is observed with *mio*, *seh1* influences the ability of the oocyte to maintain the meiotic cycle and oocyte fate beyond the germarium.

As Seh1 has been implicated in a variety of cellular functions, there are several possibilities as to how it might influence oocyte development and meiotic progression. First, Seh1 might act at the NPC to regulate the nucleocytoplasmic transport of specific molecules required for oocyte differentiation and growth. Second, Seh1 might regulate the activity of Mtor and/or other nucleoporins that have recently been implicated in transcriptional regulation (Vaquerizas et al., 2010). Finally, consistent with the alterations in mitotic cyst division and Orb localization, Seh1 might directly influence the organization and/or function of microtubules within ovarian cysts. Currently, we favor the third model because it is the most congruent with previous observations on the role of Seh1 in other organisms as well as with our own data.

We have shown that Mio and Seh1 are present in a stable complex and that both proteins are dispensable for somatic development but are required for the development of the mature egg. Additionally, we find that Seh1 is required for Mio protein stability. In the *seh1* mutant background, Mio protein levels are reduced dramatically. Furthermore, depleting *seh1* via RNAi in S2 tissue culture cells results in a rapid reduction in Mio protein levels. These results suggest the following simple model. Seh1 influences oocyte growth and the maintenance of the oocyte fate through its ability to promote the stability of the Mio protein. In the absence of Seh1, Mio protein levels fall, resulting in a *mio*-like phenotype. However, two lines of evidence suggest that Mio and Seh1 have a more complex interaction. First, overexpressing *mio* in the *seh1* mutant background fails to rescue the *seh1* phenotype. This failure to rescue is observed even though the *seh1* $^{\Delta 15}$*; UAS-mio* ovaries have high levels of Mio protein in the germline. This strongly suggests that the *seh1* ovarian phenotype is not due solely to the instability of the Mio protein in the absence of Seh1. Second, *seh1* acts as a strong dominant suppressor of the *mio* 16-nurse-cell phenotype. A possible model to explain this counterintuitive result is that *mio* and *seh1* act in opposing directions to regulate a common pathway that is crucial for the maintenance of the oocyte fate. Misregulation of this common pathway by either *mio* or *seh1* could result in the reversion of the oocyte to the default state of nurse cell.

In the future, studies of Mio and Seh1 will help elucidate the pathways that drive oocyte development and meiotic progression and contribute to our understanding of how individual NPC components drive tissue-specific differentiation.

Acknowledgements

We thank Valerie Doye, Katrina Katsani and the Bloomington Stock Center for antibodies and stocks. We thank Eva Decotto and Katrina Katsani for comments on the manuscript. This research was supported by the intramural program of the Eunice Kennedy-Shriver National Institute of Child Health and Human Development at the National Institutes of Health. Deposited in PMC for release after 12 months.

Competing interests statement

The authors declare no competing financial interests.

Supplementary material

Supplementary material for this article is available at
http://dev.biologists.org/lookup/suppl/doi:10.1242/dev.057372/-/DC1

References

Aitchison, J. D., Blobel, G. and Rout, M. P. (1995). Nup120p: a yeast nucleoporin required for NPC distribution and mRNA transport. *J. Cell Biol.* **131**, 1659-1675.

Bai, S. W., Rouquette, J., Umeda, M., Faigle, W., Loew, D., Sazer, S. and Doye, V. (2004). The fission yeast Nup107-120 complex functionally interacts with the small GTPase Ran/Spi1 and is required for mRNA export, nuclear pore distribution, and proper cell division. *Mol. Cell. Biol.* **24**, 6379-6392.

Belgareh, N., Rabut, G., Bai, S. W., van Overbeek, M., Beaudouin, J., Daigle, N., Zatsepina, O. V., Pasteau, F., Labas, V., Fromont-Racine, M. et al. (2001). An evolutionarily conserved NPC subcomplex, which redistributes in part to kinetochores in mammalian cells. *J. Cell Biol.* **154**, 1147-1160.

Carpenter, A. (1981). EM autoradiographic evidence that DNA synthesis occurs at recombination nodules during meiosis. *Chromosoma* **83**, 59-80.

Chintapalli, V. R., Wang, J. and Dow, J. A. (2007). Using FlyAtlas to identify better Drosophila melanogaster models of human disease. *Nat. Genet.* **39**, 715-720.

Christerson, L. B. and McKearin, D. M. (1994). orb is required for anteroposterior and dorsoventral patterning during Drosophila oogenesis. *Genes Dev.* **8**, 614-628.

Cordes, V. C., Rackwitz, H. R. and Reidenbach, S. (1997). Mediators of nuclear protein import target karyophilic proteins to pore complexes of cytoplasmic annulate lamellae. *Exp. Cell Res.* **237**, 419-433.

Cox, D. N., Lu, B., Sun, T. Q., Williams, L. T. and Jan, Y. N. (2001a). Drosophila par-1 is required for oocyte differentiation and microtubule organization. *Curr. Biol.* **11**, 75-87.

Cox, D. N., Seyfried, S. A., Jan, L. Y. and Jan, Y. N. (2001b). Bazooka and atypical protein kinase C are required to regulate oocyte differentiation in the Drosophila ovary. *Proc. Natl. Acad. Sci. USA* **98**, 14475-14480.

de Cuevas, M. and Spradling, A. C. (1998). Morphogenesis of the Drosophila fusome and its implications for oocyte specification. *Development* **125**, 2781-2789.

de Cuevas, M., Lee, J. K. and Spradling, A. C. (1996). alpha-spectrin is required for germline cell division and differentiation in the Drosophila ovary. *Development* **122**, 3959-3968.

de Cuevas, M., Lilly, M. A. and Spradling, A. C. (1997). Germline cyst formation in Drosophila. *Annu. Rev. Genet.* **31**, 405-428.

Dienstbier, M., Boehl, F., Li, X. and Bullock, S. L. (2009). Egalitarian is a selective RNA-binding protein linking mRNA localization signals to the dynein motor. *Genes Dev.* **23**, 1546-1558.

Dimaano, C., Ball, J. R., Prunuske, A. J. and Ullman, K. S. (2001). RNA association defines a functionally conserved domain in the nuclear pore protein Nup153. *J. Biol. Chem.* **276**, 45349-45357.

Fahrenkrog, B., Koser, J. and Aebi, U. (2004). The nuclear pore complex: a jack of all trades? *Trends Biochem. Sci.* **29**, 175-182.

Fichelson, P., Jagut, M., Lepanse, S., Lepesant, J. A. and Huynh, J. R. (2010). lethal giant larvae is required with the par genes for the early polarization of the Drosophila oocyte. *Development* **137**, 815-824.

Golic, K. G. and Golic, M. M. (1996). Engineering the Drosophila genome: chromosome rearrangements by design. *Genetics* **144**, 1693-1711.

Grieder, N. C., de Cuevas, M. and Spradling, A. C. (2000). The fusome organizes the microtubule network during oocyte differentiation in Drosophila. *Development* **127**, 4253-4264.

Hase, M. E. and Cordes, V. C. (2003). Direct interaction with nup153 mediates binding of Tpr to the periphery of the nuclear pore complex. *Mol. Biol. Cell* **14**, 1923-1940.

Hendzel, M. J., Wei, Y., Mancini, M. A., Van Hooser, A., Ranalli, T., Brinkley, B. R., Bazett-Jones, D. P. and Allis, C. D. (1997). Mitosis-specific phosphorylation of histone H3 initiates primarily within pericentromeric heterochromatin during G2 and spreads in an ordered fashion coincident with mitotic chromosome condensation. *Chromosoma* **106**, 348-360.

Hetzer, M. W., Walther, T. C. and Mattaj, I. W. (2005). Pushing the envelope: structure, function, and dynamics of the nuclear periphery. *Annu. Rev. Cell Dev. Biol.* **21**, 347-380.

Hong, A., Lee-Kong, S., Iida, T., Sugimura, I. and Lilly, M. A. (2003). The p27cip/kip ortholog dacapo maintains the Drosophila oocyte in prophase of meiosis I. *Development* **130**, 1235-1242.

Huynh, J. R. and St Johnston, D. (2000). The role of BicD, Egl, Orb and the microtubules in the restriction of meiosis to the Drosophila oocyte. *Development* **127**, 2785-2794.

Huynh, J. R. and St Johnston, D. (2004). The origin of asymmetry: early polarisation of the Drosophila germline cyst and oocyte. *Curr. Biol.* **14**, R438-R449.

Huynh, J. R., Petronczki, M., Knoblich, J. A. and St Johnston, D. (2001a). Bazooka and PAR-6 are required with PAR-1 for the maintenance of oocyte fate in Drosophila. *Curr. Biol.* **11**, 901-906.

Huynh, J. R., Shulman, J. M., Benton, R. and St Johnston, D. (2001b). PAR-1 is required for the maintenance of oocyte fate in Drosophila. *Development* **128**, 1201-1209.

Iida, T. and Lilly, M. A. (2004). missing oocyte encodes a highly conserved nuclear protein required for the maintenance of the meiotic cycle and oocyte identity in Drosophila. *Development* **131**, 1029-1039.

Katsani, K. R., Karess, R. E., Dostatni, N. and Doye, V. (2008). In vivo dynamics of Drosophila nuclear envelope components. *Mol. Biol. Cell* **19**, 3652-3666.

Krasnow, M. A., Saffman, E. E., Kornfeld, K. and Hogness, D. S. (1989). Transcriptional activation and repression by Ultrabithorax proteins in cultured Drosophila cells. *Cell* **57**, 1031-1043.
Krull, S., Thyberg, J., Bjorkroth, B., Rackwitz, H. R. and Cordes, V. C. (2004). Nucleoporins as components of the nuclear pore complex core structure and Tpr as the architectural element of the nuclear basket. *Mol. Biol. Cell* **15**, 4261-4277.
Lantz, V., Chang, J. S., Horabin, J. I., Bopp, D. and Schedl, P. (1994). The Drosophila orb RNA-binding protein is required for the formation of the egg chamber and establishment of polarity. *Genes Dev.* **8**, 598-613.
Lin, H., Yue, L. and Spradling, A. C. (1994). The Drosophila fusome, a germline-specific organelle, contains membrane skeletal proteins and functions in cyst formation. *Development* **120**, 947-956.
Lince-Faria, M., Maffini, S., Orr, B., Ding, Y., Claudia, F., Sunkel, C. E., Tavares, A., Johansen, J., Johansen, K. M. and Maiato, H. (2009). Spatiotemporal control of mitosis by the conserved spindle matrix protein Megator. *J. Cell Biol.* **184**, 647-657.
Loiodice, I., Alves, A., Rabut, G., Van Overbeek, M., Ellenberg, J., Sibarita, J. B. and Doye, V. (2004). The entire Nup107-160 complex, including three new members, is targeted as one entity to kinetochores in mitosis. *Mol. Biol. Cell* **15**, 3333-3344.
Mahowald, A. P. and Strassheim, J. M. (1970). Intercellular migration of centrioles in the germarium of Drosophila melanogaster. An electron microscopic study. *J. Cell Biol.* **45**, 306-320.
Maiato, H., Sunkel, C. E. and Earnshaw, W. C. (2003). Dissecting mitosis by RNAi in Drosophila tissue culture cells. *Biol. Proced. Online* **5**, 153-161.
McKearin, D. (1997). The Drosophila fusome, organelle biogenesis and germ cell differentiation: if you build it... *BioEssays* **19**, 147-152.
Mendjan, S., Taipale, M., Kind, J., Holz, H., Gebhardt, P., Schelder, M., Vermeulen, M., Buscaino, A., Duncan, K., Mueller, J. et al. (2006). Nuclear pore components are involved in the transcriptional regulation of dosage compensation in Drosophila. *Mol. Cell* **21**, 811-823.
Mishra, R. K., Chakraborty, P., Arnaoutov, A., Fontoura, B. M. and Dasso, M. (2010). The Nup107-160 complex and gamma-TuRC regulate microtubule polymerization at kinetochores. *Nat. Cell Biol.* **12**, 165-169.
Navarro, C., Puthalakath, H., Adams, J. M., Strasser, A. and Lehmann, R. (2004). Egalitarian binds dynein light chain to establish oocyte polarity and maintain oocyte fate. *Nat. Cell Biol.* **6**, 427-435.
Orjalo, A. V., Arnaoutov, A., Shen, Z., Boyarchuk, Y., Zeitlin, S. G., Fontoura, B., Briggs, S., Dasso, M. and Forbes, D. J. (2006). The Nup107-160 nucleoporin complex is required for correct bipolar spindle assembly. *Mol. Biol. Cell* **17**, 3806-3818.
Page, S. L. and Hawley, R. S. (2001). c(3)G encodes a Drosophila synaptonemal complex protein. *Genes Dev.* **15**, 3130-3143.
Pepling, M. E. (2006). From primordial germ cell to primordial follicle: mammalian female germ cell development. *Genesis* **44**, 622-632.
Pepling, M. E., de Cuevas, M. and Spradling, A. C. (1999). Germline cysts: a conserved phase of germ cell development? *Trends Cell Biol.* **9**, 257-262.
Platani, M., Santarella-Mellwig, R., Posch, M., Walczak, R., Swedlow, J. R. and Mattaj, I. W. (2009). The Nup107-160 nucleoporin complex promotes mitotic events via control of the localization state of the chromosome passenger complex. *Mol. Biol. Cell* **20**, 5260-5275.
Qi, H., Rath, U., Wang, D., Xu, Y. Z., Ding, Y., Zhang, W., Blacketer, M. J., Paddy, M. R., Girton, J., Johansen, J. et al. (2004). Megator, an essential coiled-coil protein that localizes to the putative spindle matrix during mitosis in Drosophila. *Mol. Biol. Cell* **15**, 4854-4865.
Roper, K. and Brown, N. H. (2004). A spectraplakin is enriched on the fusome and organizes microtubules during oocyte specification in Drosophila. *Curr. Biol.* **14**, 99-110.
Rorth, P. (1998). Gal4 in the Drosophila female germline. *Mech. Dev.* **78**, 113-118.
Ryder, E., Blows, F., Ashburner, M., Bautista-Llacer, R., Coulson, D., Drummond, J., Webster, J., Gubb, D., Gunton, N., Johnson, G. et al. (2004). The DrosDel collection: a set of P-element insertions for generating custom chromosomal aberrations in Drosophila melanogaster. *Genetics* **167**, 797-813.
Tautz, D. and Pfeifle, C. (1989). A non-radioactive in situ hybridization method for the localization of specific RNAs in Drosophila embryos reveals translational control of the segmentation gene hunchback. *Chromosoma* **98**, 81-85.
Theurkauf, W. E., Alberts, B. M., Jan, Y. N. and Jongens, T. A. (1993). A central role for microtubules in the differentiation of Drosophila oocytes. *Development* **118**, 1169-1180.
Thibault, S. T., Singer, M. A., Miyazaki, W. Y., Milash, B., Dompe, N. A., Singh, C. M., Buchholz, R., Demsky, M., Fawcett, R., Francis-Lang, H. L. et al. (2004). A complementary transposon tool kit for Drosophila melanogaster using P and piggyBac. *Nat. Genet.* **36**, 283-287.
Vaquerizas, J. M., Suyama, R., Kind, J., Miura, K., Luscombe, N. M. and Akhtar, A. (2010). Nuclear pore proteins nup153 and megator define transcriptionally active regions in the Drosophila genome. *PLoS Genet.* **6**, e1000846.
Wozniak, R., Burke, B. and Doye, V. (2010). Nuclear transport and the mitotic apparatus: an evolving relationship. *Cell. Mol. Life Sci.* **67**, 2215-2230.
Zuccolo, M., Alves, A., Galy, V., Bolhy, S., Formstecher, E., Racine, V., Sibarita, J. B., Fukagawa, T., Shiekhattar, R., Yen, T. et al. (2007). The human Nup107-160 nuclear pore subcomplex contributes to proper kinetochore functions. *EMBO J.* **26**, 1853-1864.